Turkish Journal of Computer and Mathematics Education Vol.12 No.13 (2021), 3293-3299

Research Article

Dead-beat Control for Polysolenoid Linear Motor

Nguyen Hong Quang[a,*], Nguyen Phung Quang[b], and Vo Thanh Ha[c]
[a]Thai Nguyen University of Technology, Viet Nam
[b]Hanoi University of Science and Technology, Viet Nam
[c]University of Transport and Communications, Vietnam

Article History: Received: 11 January 2021; Revised: 12 February 2021; Accepted: 27 March 2021; Published online: 4 June 2021

Abstract: The field-oriented control (FOC) has been successfully applied to permanently excited linear motors in high-quality drive systems. With this control method, the system kinematics is enhanced, and the upper limits of thrust and acceleration are increased. Accordingly, the accuracy of the position response will be improved. For the FOC method, the stator current control loop of the system plays a major role in the quality of the system. This paper introduces a current vector dead-beat control for Polysolenoid linear motors with fast, accurate, and decoupling characteristics. Numerical simulations demonstrate the advantage of the proposed algorithm.

Key words: Linear Motor, Polysolenoid Linear Motor, PMSLM, FOC, Dead-Beat Control.

1. Introduction

Linear motors produce direct linear motion without the need for intermediate mechanisms such as belts and screws. The basic principle of a linear motor is to generate linear motion directly from electrical energy, wherein the part that produces the rectilinear motion can be a primary part (stator side) or a secondary part (rotor side) [1-4]. Polysolenoid linear motor is a particular case of permanently excited linear motor, with tubular construction. The working principle of the Polysolenoid motor has been presented in [1-5].

For control of permanently excited synchronous linear motors, different techniques have been presented. Model predictive control [6-8], flatness-based control [9], and exact linearization controller [10] were proposed to decouple the controller of the nonlinear model in the transition state space. In [11], a state observer was developed to observe the velocity and position to compensate the control signal with uncertainty affecting the system. In [12-15], sliding mode control was designed to control the position of linear motors. In [16], a fuzzy PID controller was implemented for the speed loop to improve system response performance. The study in [17] combined the advantages of adaptive control and fuzzy PID to reduce the speed overshoot. Integrated iterative learning and a PID controller to control the position with the imprecise model of the linear motor were introduced [18].

These studies mentioned above, however, only focus on reducing the steady-state position error. Meanwhile, the issue of shortening the transient time has not been adequately addressed. To improve the transient time of the FOC control system, the current loop with the fast kinematics plays a decisive role [19, 20]. This paper introduces a current dead-bead control, ensuring fast and accurate response as well as eliminating the interaction between magnetization and force generation.

2. Mathematical Model of the Polysolenoid Motor

The Polysoleniod motor works on the principle of electromagnetic induction, with the primary part being two coils placed 90 degrees apart as shown in Figure 1. The mathematical model of the motor is given as [7]:

$$\begin{cases} \dfrac{di_{sd}}{dt} = -\dfrac{R_s}{L_{sd}} i_{sd} + \left(\dfrac{2\pi p}{\tau} v\right)\dfrac{L_{sq}}{L_{sd}} i_{sq} + \dfrac{u_{sd}}{L_{sd}} \\ \dfrac{di_{sq}}{dt} = -\dfrac{R_s}{L_{sq}} i_{sq} - \left(\dfrac{2\pi}{\tau} v\right)\dfrac{L_{sd}}{L_{sq}} i_{sd} - \left(\dfrac{2\pi p}{p\tau} v\right)\dfrac{\psi_p}{L_{sq}} + \dfrac{u_{sq}}{L_{sq}} \\ \dfrac{dv}{dt} = \dfrac{2\pi p}{\tau}\left(\psi_p + \left(L_{sd} - L_{sq}\right) i_{sd}\right) i_{sq} - \dfrac{1}{m} F_c \\ \dfrac{dx}{dt} = v \end{cases} \quad (1)$$

In a linear motor, the current loop has the same properties as a force loop. The responsiveness of the current loop, which is the innermost loop, is decisive to the control quality of the system.

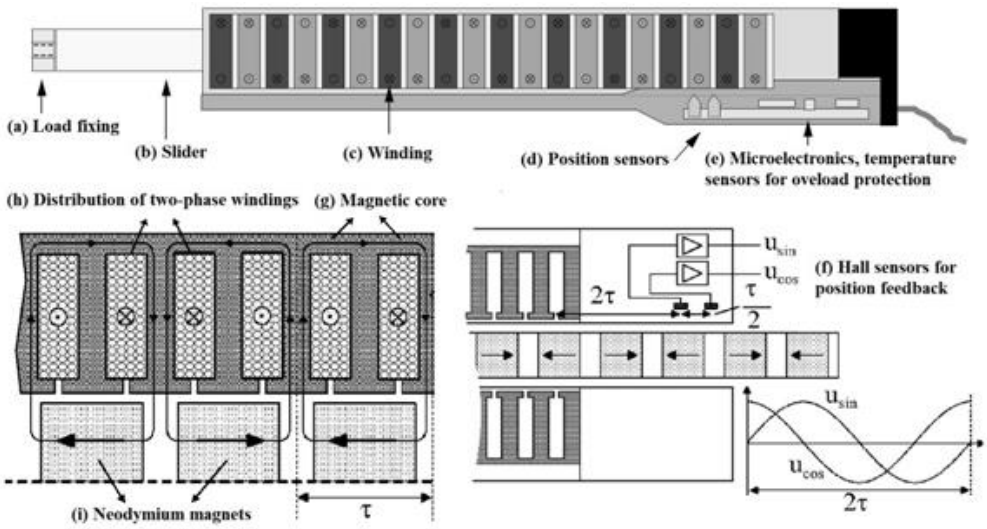

Figure 1: Polysolenoid Typed Permanent Excitation Linear Motor [1,2].

3.Design of Current Controller

From the continuous-time model of the motor (1), the descrete-time state model of the current on the dq coordinate system is derived as below:

$$\frac{d\mathbf{i}_{dq}}{dt} = \mathbf{A}\mathbf{i}_{dq} + \mathbf{B}\mathbf{u}_{dq} + \mathbf{N}\mathbf{i}_{dq}\omega_e + \mathbf{S}\psi_p\omega_e, \quad (2)$$

Where

$$\mathbf{i}_{dq}{}^T = \begin{bmatrix} i_d & i_q \end{bmatrix}, \mathbf{u}_{dq}{}^T = \begin{bmatrix} u_d & u_q \end{bmatrix}$$

$$\mathbf{A} = \begin{bmatrix} -\frac{R_s}{L_d} & 0 \\ 0 & -\frac{R_s}{L_q} \end{bmatrix}, \ \mathbf{B} = \begin{bmatrix} \frac{1}{L_d} & 0 \\ 0 & \frac{1}{L_q} \end{bmatrix}, \mathbf{N} = \begin{bmatrix} 0 & \frac{L_q}{L_d} \\ -\frac{L_d}{L_q} & 0 \end{bmatrix}, \mathbf{S} = \begin{bmatrix} 0 \\ -\frac{1}{L_q} \end{bmatrix}.$$

By using the first-order Euler approximation, equation (2) is rewritten as

$$\mathbf{i}_{dq}(k+1) = \mathbf{\Phi}\mathbf{i}_{dq}(k) + \mathbf{H}\mathbf{u}_{dq}(k) + \mathbf{h}\psi_p \quad (3)$$

in which

$$\mathbf{\Phi} = \mathbf{I} + T_s\mathbf{A} + T_s\mathbf{N}\omega_e(k) = \begin{bmatrix} \Phi_{11} & \Phi_{12} \\ \Phi_{21} & \Phi_{22} \end{bmatrix} = \begin{bmatrix} 1 - T_s R_s / L_d & T_s L_q \omega_e(k) / L_d \\ -T_s L_d \omega_e(k) / L_q & 1 - T_s R_s / L_q \end{bmatrix},$$

$$\mathbf{H} = T_s\mathbf{B} = \begin{bmatrix} H_{11} & 0 \\ 0 & H_{22} \end{bmatrix} = \begin{bmatrix} T_s / L_d & 0 \\ 0 & T_s / L_q \end{bmatrix}, \ \mathbf{h} = \begin{bmatrix} h_1 \\ h_2 \end{bmatrix} = \begin{bmatrix} 0 \\ -T_s\omega_e(k) / L_q \end{bmatrix}$$

Where T_s is the current sampling time. For electric motors, the kinetics of the current is much faster than the speed and Ts is very small, so the composition $\omega_e(k)$ in the matrices $\mathbf{\Phi}$, $\mathbf{h}$ is assumed to be constant for the time period T_s.

Transforming (3) into z domain yields:

$$z\mathbf{i}_{dq}(z) = \mathbf{\Phi}\mathbf{i}_{dq}(z) + \mathbf{H}\mathbf{u}_{dq}(z) + \mathbf{h}\psi_p \quad (4)$$

To eliminate the influence of the flux component in equation (4), the control voltage is designed as

$$\mathbf{u}_{dq}(k) = \mathbf{H}^{-1}\left[\mathbf{x}(k-1) - \mathbf{h}\psi_p\right] \quad (5)$$

Where $\mathbf{x}(k)$ is the output of the controller, $\mathbf{x}(k-1)$ represents a hardware-induced one-cycle delay. To calculate the voltage of the current cycle $\mathbf{u}_{dq}(k)$, we use the output of the previous cycle $\mathbf{x}(k-1)$.

Substituting (5) into (4), we get the compensated current model as

$$(z\mathbf{I} - \mathbf{\Phi})\mathbf{i}_{dq}(z) = z^{-1}\mathbf{x}(z) \quad (6)$$

The adjustment equation in z-domain is as below:

$$\mathbf{x}(z) = \mathbf{R}_\mathbf{I}(z)\left[\mathbf{i}^*_{dq}(z) - \mathbf{i}_{dq}(z)\right] \quad (7)$$

Where $\mathbf{R_I}(z)$ is the current controller to be designed.

Choose a polynomial matrix as

$$\mathbf{P}\left(z^{-1}\right)=\begin{bmatrix} P_1\left(z^{-1}\right) & 0 \\ 0 & P_2\left(z^{-1}\right) \end{bmatrix} \quad (8)$$

We select a matrix $\mathbf{R_I}$ as follow and prove that the controller according to (7) produces a finite response of the closed system:

$$\mathbf{R_I}\left(z^{-1}\right)=\left(z\mathbf{I}-\mathbf{\Phi}\right)\mathbf{P}\left(z^{-1}\right)\left[\mathbf{I}-z^{-1}\mathbf{P}\left(z^{-1}\right)\right]^{-1} \quad (9)$$

To prove, replacing (9), (7) in (6) we get:

$$\left(z\mathbf{I}-\mathbf{\Phi}\right)\mathbf{i}_{dq}(z)=z^{-1}\left(z\mathbf{I}-\mathbf{\Phi}\right)\mathbf{P}\left(z^{-1}\right)\left[\mathbf{I}-z^{-1}\mathbf{P}\left(z^{-1}\right)\right]^{-1}\left[\mathbf{i}^{*}_{dq}(z)-\mathbf{i}_{dq}(z)\right] \quad (10)$$

Since the matrix $\left(z\mathbf{I}-\mathbf{\Phi}\right)$ is invertible:

$$\det\left(z\mathbf{I}-\mathbf{\Phi}\right)=\left(z-1+T_s\frac{R_s}{L_{sd}}\right)^2+\left(T_s\frac{L_{sq}}{L_{sd}}\omega_e\right)^2>0$$

From (10) we have:

$$\mathbf{i}_{dq}(z)=z^{-1}\mathbf{P}\left(z^{-1}\right)\left[\mathbf{I}-z^{-1}\mathbf{P}\left(z^{-1}\right)\right]^{-1}\left[\mathbf{i}^{*}_{dq}(z)-\mathbf{i}_{dq}(z)\right] \quad (11)$$

Define $\mathbf{G}_h\left(z^{-1}\right)=z^{-1}\mathbf{P}\left(z^{-1}\right)\left[\mathbf{I}-z^{-1}\mathbf{P}\left(z^{-1}\right)\right]^{-1}$ is the transfer function matrix, we see that $\mathbf{G}_h\left(z^{-1}\right)$ is in the diagonal form:

$$\mathbf{G}_h\left(z^{-1}\right)=\begin{bmatrix} \dfrac{z^{-1}P_1\left(z^{-1}\right)}{1-z^{-1}P_1\left(z^{-1}\right)} & 0 \\ 0 & \dfrac{z^{-1}P_2\left(z^{-1}\right)}{1-z^{-1}P_2\left(z^{-1}\right)} \end{bmatrix} \quad (12)$$

Moving $\mathbf{i}_{dq}(z)$ in (11) from right to left in equation, we get:

$$\mathbf{i}_{dq}(z)=z^{-1}\mathbf{P}\left(z^{-1}\right)\mathbf{i}^{*}_{dq}(z) \quad (13)$$

In (13), due to the matrix $\mathbf{P}$ is chosen diagonally, the proposed controller (6) has ensured the decoupling between i_{sd} and i_{sq}. Furthermore, since P_1, P_2 have the corresponding degree n_1, n_2, the response of the closed system according to (13) will be finite after n_1+1, n_2+1 periods, respectively.

To eliminate control error, the closed-system transfer function must be equal to the unit matrix $\mathbf{I}$ at the steady state. From (13) we have:

$$P_1(1)=P_2(1)=1 \quad (14)$$

That is, the sum of the coefficients P_1, P_2 must equal one.

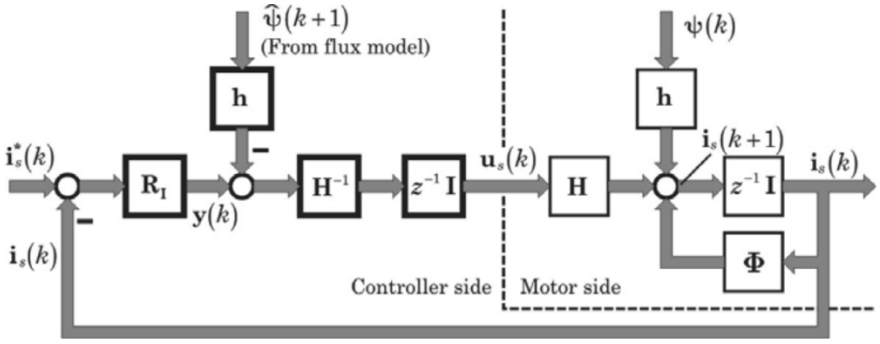

Figure 2: Block Diagram of Stator Current Dead-Beat Control on Coordinates Coupled with Rotor Magnetic Flux.

Substituting (8) into (9), we obtain the differential equation of the controller as below:

$$\mathbf{R_I}\left(z^{-1}\right)=\begin{bmatrix}\dfrac{\left(z-\Phi_{11}\right)P_1\left(z^{-1}\right)}{1-z^{-1}P_1\left(z^{-1}\right)} & \dfrac{-\Phi_{12}P_2\left(z^{-1}\right)}{1-z^{-1}P_2\left(z^{-1}\right)}\\ \dfrac{-\Phi_{21}P_1\left(z^{-1}\right)}{1-z^{-1}P_1\left(z^{-1}\right)} & \dfrac{\left(z-\Phi_{22}\right)P_2\left(z^{-1}\right)}{1-z^{-1}P_2\left(z^{-1}\right)}\end{bmatrix} \quad (15)$$

From the component $\left(z-\Phi_{11}\right)P_1\left(z^{-1}\right)$ in (15), we see that the free component in $P_1\left(z^{-1}\right)$ must be zero to ensure the feasibility of equation (3).

To create the same kinematics for both the d and q axes, we choose:

$$P_1\left(z^{-1}\right)=P_2\left(z^{-1}\right)=P\left(z^{-1}\right)=\sum_{i=1}^{N}p_i z^{-i} \quad (16)$$

Accordingly, the output of the controller (7) has the following form:

$$\begin{aligned}x_d\left(z^{-1}\right)&=\frac{\left(z-\Phi_{11}\right)P\left(z^{-1}\right)}{1-z^{-1}P\left(z^{-1}\right)}e_d\left(z^{-1}\right)-\frac{\Phi_{12}P\left(z^{-1}\right)}{1-z^{-1}P\left(z^{-1}\right)}e_q\left(z^{-1}\right)\\ x_q\left(z^{-1}\right)&=\frac{\left(z-\Phi_{22}\right)P\left(z^{-1}\right)}{1-z^{-1}P\left(z^{-1}\right)}e_q\left(z^{-1}\right)-\frac{\Phi_{21}P\left(z^{-1}\right)}{1-z^{-1}P\left(z^{-1}\right)}e_d\left(z^{-1}\right)\end{aligned} \quad (17)$$

Where $e_d=i_d^*-i_d, e_q=i_q^*-i_q$. To implement the algorithm, (17) is written in the form of the differential equation as

$$\begin{aligned}x_d\left(k\right)&=\sum_{i=1}^{N}l_i\left[x_d\left(k-i-1\right)+e_d\left(k-i+1\right)-\Phi_{11}e_d\left(k-i\right)-\Phi_{12}e_q\left(k-i\right)\right]\\ x_q\left(k\right)&=\sum_{i=1}^{N}l_i\left[x_q\left(k-i-1\right)+e_q\left(k-i+1\right)-\Phi_{22}e_q\left(k-i\right)-\Phi_{21}e_d\left(k-i\right)\right]\end{aligned} \quad (18)$$

The stator voltage is computed according to (5) as

$$\begin{aligned}u_d\left(k+1\right)&=H_{11}^{-1}\left[x_d\left(k\right)-h_1\psi_p\right]\\ u_q\left(k+1\right)&=H_{22}^{-1}\left[x_q\left(k\right)-h_2\psi_p\right]\end{aligned} \quad (19)$$

Kinematics for both the d and q axes, we choose:

4.Simulation Results

This section presents simulation result of the designed control algorithm. The motor parameters are given in Table. 1. To evaluate the performance of the dead-beat current regulator, an incremental reference with outer loop sampling time T_{ws} = 5Ts, N = 2. Responses of the dead-beat controller designed in (19) are shown in Figures 3 and 4. These figures depicts that the *iq* and *id* current values are controlled completely independently, demonstrating the decoupling capability of the controller. The responseability of the controller within N = 2 sampling cycles validates the correctness of the design method.

Table 1: Motor Parameters

Motor Parameters	Symbol	Value	Unit
d Axis Stator Inductance	L_{sd}	1.4	mH
q Axis Stator Inductance	L_{sq}	1.4	mH
Stator Resistance	R_s	10.3	Ω
Rotor Flux	ψ_p	0.035	Wb
Number of Pole Pair	z_p	2	
Pole Step	τ_p	0.02	m

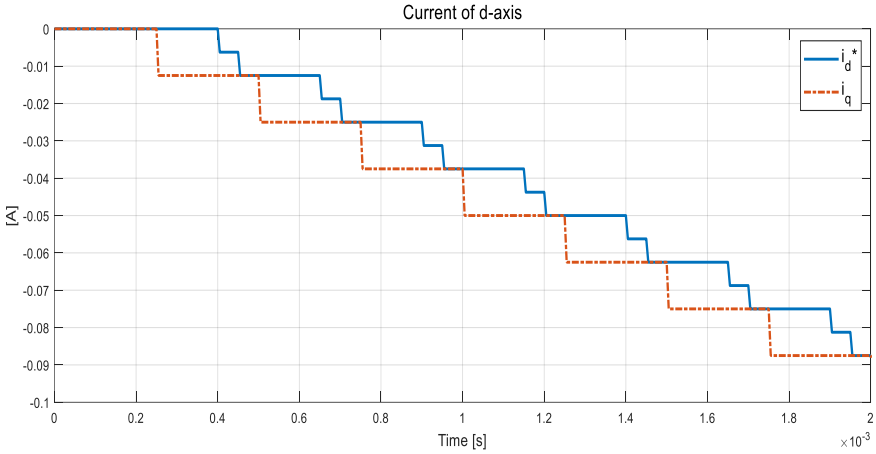

Figure 3: The d-Axis Current Response of the Deadbeat Controller.

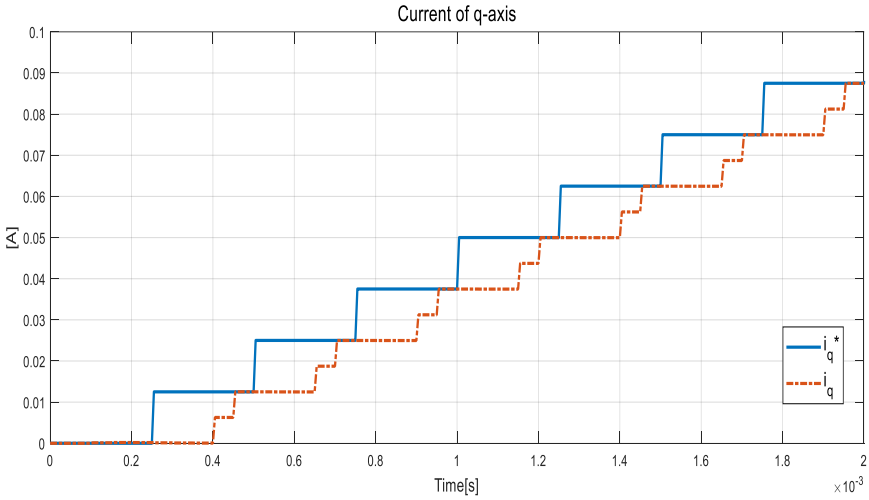

Figure 4: The q-Axis Current Response of the Deadbeat Controller.

With the advantage of fast current response, a cascade control structure is designed as shown in Figure 5 to validate the ability of the controller to work with a real system. Parameters of the speed and position regulators are given in Table 2. For the designed control structure, the velocity and position responses, as depicted in Figures 6, 7, 10, and 11, show the excellent workability of the current controller with different outer loop controllers. The speed and position regulator parameters can be varied over a wide range in response to different loads and trajectories. In the simulation case, the objective is to reduce the tracking error, as demonstrated in Figures 8 and 9. This mainly depends on the response of the current controller. Therefore, the dead-beat controller can work well with different outer loop controllers.

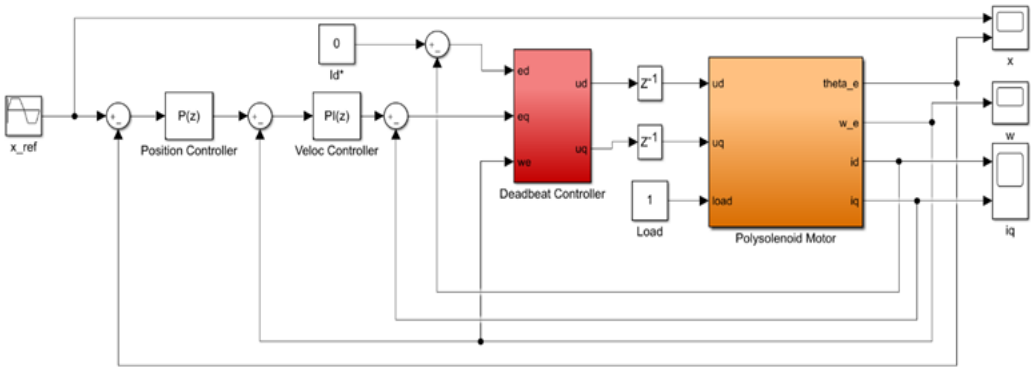

Figure 5: Structure of the Control System.

Table 2: Control Parameters

Control Parameters	Symbol	Controller 1	Controller 2
Proportional Gain of the Position Controller	k_{pp}	40	100
Proportional Gain of the Speed Controller	$k_{p\omega}$	0.1	0.1
Integral Gain of the Speed Controller	$k_{i\omega}$	10	20

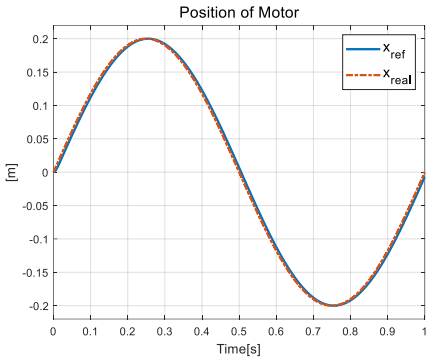

Figure 6: Position Response of the Outer Loop Controller 1.

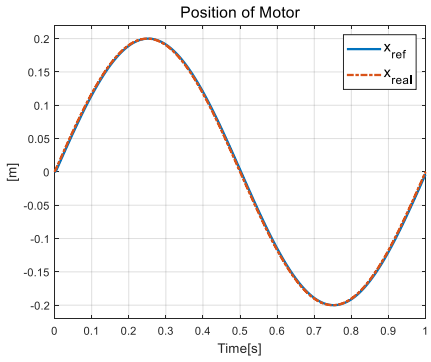

Figure 7: Position Response of the Outer Loop Controller 2.

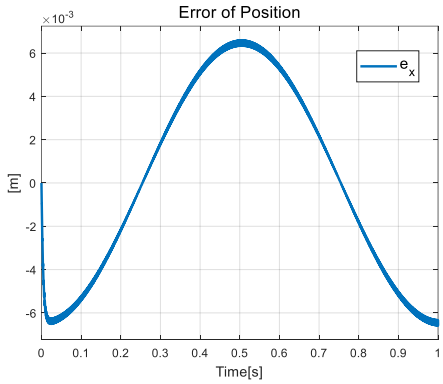

Figure 8: Position Error of the Outer Loop Controller 1.

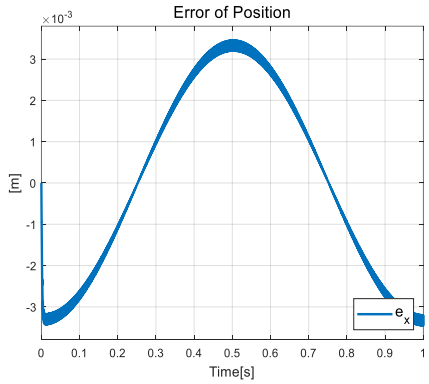

Figure 9: Position Error of the Outer Loop Controller 2.

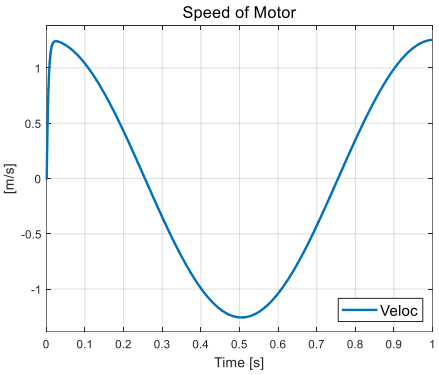

Figure 10: Speed Response of the Outer Loop Controller 1.

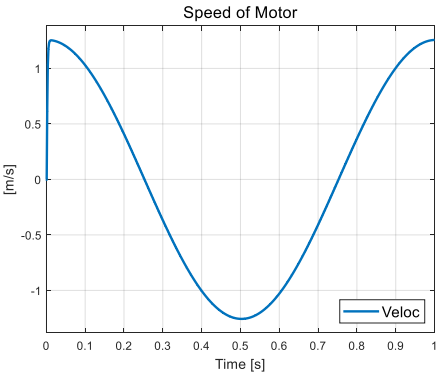

Figure 11: Speed Response of the Outer Loop Controller 2.

5. Conclusions

The dead-beat control method designed for the Polysolenoid motor current loop has ensured accurately impose of the stator current after a finite number of sampling cycles. Besides, this method provides the ability to separate two current components on the dq-coordinate system. The d-axis component generates flux, and the q-axis part generates thrust in a linear motor. This is validated by successfully controlling a current loop with a finite response time and no overshoot, which increases the dynamics and reduces the response time of the system. In the ongoing study, experimental validation will be conducted to validate the control algorithm in practice.

Acknowledgments

This research was funded by Thai Nguyen University of Technology, No. 666, 3/2 street, Thai Nguyen,Viet Nam.

References

1. Ausderau, D. (2004). Polysolenoid-Linearantrieb mit genutetem Stator(Doctoral dissertation, ETH Zurich).
2. Gieras, J. F. (2018). Linear Electric Motors. In Electric Power Generation, Transmission, and Distribution: The Electric Power Engineering Handbook (pp. 34-1). CRC Press.
3. Boldea, I., Tutelea, L. N., Xu, W., & Pucci, M. (2017). Linear electric machines, drives, and MAGLEVs: an overview. IEEE Transactions on Industrial Electronics, 65(9), 7504-7515.
4. Boldea, I. (2017). Linear Electric Machines, Drives, and MAGLEVs Handbook. CRC Press.
5. LinMot Company Home Page: Products, Linear Motors. Available online: https://linmot.com/products/linear-motors/ (accessed on 1 March 2020).
6. Quang, N. H. (2017). Multi parametric programming based model predictive control for tracking control of polysolenoid linear motor. Special issue on Measurement, Control and Automation, 19, 31-37.
7. Quang, N. H., Quang, N. P., & Hien, N. N. (2020). On tracking control problem for Polysolenoid motor model predictive approach. International Journal of Electrical & Computer Engineering (2088-8708), 10(1).
8. Nam, D. P., Quang, N. H., Hung, N. M., & Ty, N. T. (2017, July). Multi parametric programming and exact linearization based model predictive control of a permanent magnet linear synchronous motor. In 2017 International Conference on System Science and Engineering (ICSSE) (pp. 743-747). IEEE.
9. Nguyen, Q. H., Dao, N. P., Nguyen, T. T., Nguyen, H. M., Nguyen, H. N., & Vu, T. D. (2016). Flatness based control structure for polysolenoid permanent stimulation linear motors. SSRG International Journal of Electrical and Electronics Engineering, 3(12), 31-37.
10. Nguyen, Q. H., Dao, N. P., Nguyen, H. M., Nguyen, H. N., Nguyen, T. T., & Nguyen, C. P. (2017). Design an exact linearization controller for permanent stimulation synchronous linear motor polysolenoid. SSRG International Journal of Electrical and Electronics Engineering, 4(1), 7-12.
11. Nguyen, H. Q. (2020, March). Observer-Based Tracking Control for Polysolenoid Linear Motor with Unknown Disturbance Load. In Actuators (Vol. 9, No. 1, p. 23). Multidisciplinary Digital Publishing Institute.
12. Sun, G., Wu, L., Kuang, Z., Ma, Z., & Liu, J. (2018). Practical tracking control of linear motor via fractional-order sliding mode. Automatica, 94, 221-235.
13. Du, H., Chen, X., Wen, G., Yu, X., & Lü, J. (2018). Discrete-time fast terminal sliding mode control for permanent magnet linear motor. IEEE Transactions on Industrial Electronics, 65(12), 9916-9927.
14. Yang, C., Ma, T., Che, Z., & Zhou, L. (2017). An adaptive-gain sliding mode observer for sensorless control of permanent magnet linear synchronous motors. IEEE Access, 6, 3469-3478.
15. Sun, G., & Ma, Z. (2017). Practical tracking control of linear motor with adaptive fractional order terminal sliding mode control. IEEE/ASME Transactions on Mechatronics, 22(6), 2643-2653.
16. Wu, Y., Jiang, H., & Zou, M. (2012). The research on fuzzy PID control of the permanent magnet linear synchronous motor. Physics Procedia, 24, 1311-1318.
17. Hu, Q., Zhang, J., Yu, D., & Cui, J. (2007, August). Velocity control for rope-less elevator using permanent magnet linear synchronous motor with adaptive fuzzy PID. In 2007 IEEE International Conference on Automation and Logistics (pp. 2361-2366). IEEE.
18. Li, H., Sheng, H., & Shen, L. (2021, April). Iterative learning PID Controller for Permanent Magnet Linear Synchronous Motor. In Journal of Physics: Conference Series (Vol. 1852, No. 3, p. 032044). IOP Publishing.
19. Quang, N. P., & Dittrich, J. A. (2008). Vector control of three-phase AC machines (Vol. 2). Heidelberg: springer.
20. Quang, N. P., Ha, V. T., & Trung, T. V. (2018). A new control design with dead-beat behavior for stator current vector in three-phase AC drives. International Journal of Electrical and Electronics Engineering, 5(4), 1-8.